J|A|C|S

A R T I C L E S

Theoretical Calculations of Carbon–Oxygen Bond Dissociation Enthalpies of Peroxyl Radicals Formed in the Autoxidation of Lipids

Derek A. Pratt, Jeremy H. Mills, and Ned A. Porter*

Contribution from the Department of Chemistry and the Center in Molecular Toxicology, Vanderbilt University, Nashville, Tennessee 37235

Received January 15, 2003; E-mail: n.porter@vanderbilt.edu

Abstract: Theoretical calculations were carried out to provide a framework for understanding the free radical oxidation of unsaturated lipids. The carbon–hydrogen bond dissociation enthalpies (BDEs) of organic model compounds and oxidizable lipids (R–H) and the carbon–oxygen bond dissociation enthalpies of peroxyl radical intermediates (R–OO•) have been calculated. The carbon–hydrogen BDEs correlate with the rate constant for propagation of free radical autoxidation, and the carbon–oxygen BDEs of peroxyl radicals correlate with rate constants for β-fragmentation of these intermediates. Oxygen addition to intermediate carbon radicals apparently occurs preferentially at centers having the highest spin density. The calculated spin distribution therefore provides guidance about the partitioning of oxygen to delocalized carbon radicals. Where the C–H BDEs are a function of the extent of conjugation in the parent lipid and the stability of the carbon radical derived therefrom, C–OO• BDEs are also affected by hyperconjugation. This gives way to different rates of β-fragmentation of peroxyl radicals formed from oxygen addition at different sites along the same delocalized radical. We have also studied by both theory and experiment the propensity for benzylic radicals to undergo oxygen addition at their ortho and para carbons which, combined, possess an equivalent unpaired electron spin density as the benzylic position itself. We find that the intermediate peroxyl radicals in these cases have negative C–OO• BDEs and, thus, have rate constants for β-fragmentation that exceed the diffusion-controlled limit for the reaction of a carbon-centered radical with oxygen.

Introduction

The autoxidation of polyunsaturated fatty acids and esters has been the focus of intense investigation because of its potential importance in biology and medicine.[1,2] This process, shown in Scheme 1, has a slow propagation step, k_p, that involves hydrogen atom transfer to a peroxyl radical and a fast step, k_{O2}, where oxygen adds to the intermediate carbon radical. Oxygen addition is reversible for many radicals, and the rate constant for the reverse reaction, k_β, is also shown in the scheme. Product mixtures obtained from the free radical chain oxidation of diene fatty acids or esters consist principally of diene hydroperoxides, as shown in Scheme 1. Thus, free radical oxidation of linoleic acid or its esters, **1**, gives five major product diene hydroperoxides, **2**–**6**.[3,4] Two of these product hydroperoxides, **2** and **5**, are *cis, trans* dienes having hydroperoxide substitution at the 13 and 9 position of the C-18 chain. These compounds are the major products formed in linoleate oxidations in which millimolar concentrations of phenolic antioxidants (ArOH), such as α-tocopherol, are present during the reaction.

(1) (a) Marnett, L. J. *Carcinogenesis* **2000**, *21*, 361–370. (b) Sevanian, A.; Ursini, F.. *Free Radical Biol. Med.* **2000**, *29*, 306–311. (c) Spiteller, G.; Spiteller, D.; Jira, W.; Kiessling, U.; Dudda, A.; Weisser, M.; Hecht, S.; Schwarz, C. *Peroxide Chem.* **2000**, 179–208.
(2) (a) Steinburg, D.; Parhsarathy, S.; Carew, T. E.; Khoo, J. C.; Witztum, J. L. *N. Engl. J. Med.* **1989**, *320*, 915–924. (b) Chisholm, G. M.; Steinburg, D. *Free Radical Biol. Med.* **2000**, *28*, 1815–1826.
(3) Chan, H. W.-S.; Levett, G. *Lipids* **1977**, *12*, 99–104.
(4) (a) Porter, N. A. *Acc. Chem. Res.* **1986**, *19*, 262–268. (b) Porter, N. A.; Caldwell, S. E.; Mills, K. A. *Lipids* **1995**, *30*, 277–290.

**Scheme 1.** Chain Propagation Steps and Products of Linoleate Free Radical Oxidation
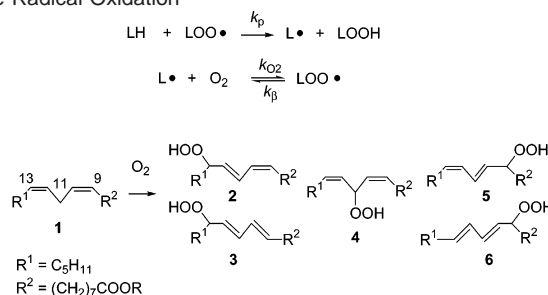
Two other hydroperoxides, **3** and **6**, having *trans, trans* diene geometry are formed in oxidations carried out in the absence of antioxidants.[5] Recently, a nonconjugated hydroperoxide, **4**, was identified as a product formed from oxidations of methyl linoleate to which ∼0.1 M α-tocopherol was added.[6]

Mechanistic studies suggest that one key to understanding product distribution in diene fatty acid oxidation is the reversibility of oxygen addition to intermediate pentadienyl radicals. Thus, as illustrated in Scheme 2, loss of oxygen from diene peroxyl radicals competes with hydrogen atom trapping of these peroxyls by phenolic antioxidants. The distribution of products derived from linoleate depends therefore on the rates of

(5) Porter, N. A.; Wujek, D. G. *J. Am. Chem. Soc.* **1984**, *106*, 2626–2629.
(6) (a) Brash, A. R. *Lipids* **2000**, *35*, 947–952. (b) Tallman, K. A.; Pratt, D. A.; Porter, N. A. *J. Am. Chem. Soc.* **2001**, *123*, 11827–11828.
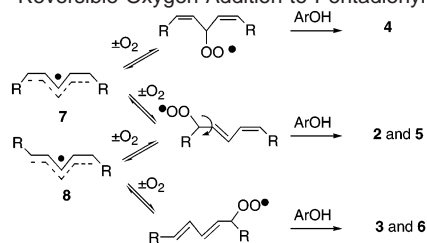
hydrogen atom transfer from ArOH to, and β-fragmentation of, intermediate peroxyls as well as on the partitioning of oxygen to the reactive sites on the delocalized radical intermediates.

Given the fundamental importance of the reactions of delocalized carbon radicals such as **7** and **8** and the peroxyl radicals formed from these species by oxygen addition to the understanding of peroxidation mechanisms, we set out to examine the important reactions of these radicals by theory. Specifically, we seek answers to the following questions: (1) What is the relative ease with which a hydrogen atom can be removed from an unsaturated lipid? One anticipates that the rate constants for hydrogen atom transfer should be related to the bond dissociation enthalpy (BDE) of the relevant C–H bond. A peroxyl radical is the partner in this reaction and peroxyl radicals have O–H BDEs that are relatively independent of structure,[7] leaving the C–H BDE uniquely relevant to the rate of the H atom transfer. (2) Where does the unpaired electron spin density reside in the delocalized intermediate carbon-centered radical, and does oxygen add preferentially to carbon centers having more spin density? (3) Finally, following the addition of oxygen to these radicals, how stable are the resulting lipid peroxyl radicals toward β-fragmentation? Given the fact that these reactions are endothermic and the reverse reaction, oxygen addition, occurs without a substantial barrier, we believe the rate constants for β-fragmentation should be uniquely dependent on the C–OO• BDE. To provides answers to these questions of interest, we report here a computational study to determine the C–H BDEs in lipids of interest, the spin density distributions in the incipient radicals formed from those lipids, and the C–OO• BDEs in the lipid peroxyl radicals derived therefrom, respectively.

Results and Discussion

Choice of Methodology. To calculate the C–H BDEs in the lipids of interest, we required a methodology that would successfully reproduce available experimental data but also be computationally tractable on the larger models of polyunsaturated systems and of their corresponding peroxyl radicals. Because of our past successes using model density functional theory (DFT) calculations employing the B3LYP density functional to predict X–H BDEs,[8] we applied these models to a short series of unsaturated hydrocarbons. The results are shown in Table 1. Results obtained by the high accuracy compound G3[9] and G3MP2[10] methods as well as some experimental data are presented alongside for comparison.

We have included methane in the series to determine the radical stabilization enthalpies (RSEs) of the substituents:

$$RSE(Y) = BDE(Y-CH_2-H) - BDE(CH_3-H) \quad (1)$$

As has been noted previously,[8] all methods agree well on this simplest case.

Although the DFT models perform well for the most part, there are some noteworthy exceptions. It has been reported elsewhere that DFT underestimates X–H BDEs (X = O, N) for compounds with increasingly weak bonds (i.e., the deviation in calculated BDEs from experimental data is larger the more stable the incipient radical).[14-17] It would appear that DFT also underestimates C–H BDEs for compounds with increasingly weak bonds as shown in Table 1 (cf. methane through to 1,4-pentadiene). Improving the quality of the model improves the agreement with experiment, especially for 1,4-pentadiene, but the HLM result of 74.2 kcal/mol is still 2.2 kcal/mol lower than the experimental value of 76.4 kcal/mol. Increasing the basis set size to 6-311++G(3df,3pd) does not improve the agreement (74.1 kcal/mol), suggesting that the basis set limit has already been reached at 6-311+G(2d,2p). Moreover, using a large correlation consistent basis set does not improve the result (74.4 by ROB3LYP/AUG-cc-pVTZ). The G3 compound method predicts 75.6 kcal/mol, also low compared to experiment but only by 0.8 kcal/mol. With only five heavy atoms in 1,4-pentadiene, we were able to push the limits of theory and perform a CBS-APNO[18] calculation of the C–H BDE. CBS-APNO finds 75.3 kcal/mol, only 1.1 kcal/mol higher than the HLM result of 74.2 kcal/mol and in good agreement with the G3 result.[19]

While all methods give values within the error of the experimentally determined C–H BDE of propene, G3 and G3MP2 give values for the C–H BDE in toluene that are 2.6 and 4.6 kcal/mol, respectively, larger than experiment (88.5 ± 1.5 kcal/mol). Even the DFT models give a C–H BDE 0.8-2.1 kcal/mol higher than experiment. Indeed, while experiment suggests that RSE(benzyl) < RSE(allyl) by only a couple tenths

(7) Luo, Y.-R. *Handbook of Bond Dissociation Energies in Organic Compounds*; CRC Press: Boca Raton, FL, 2003; pp 166–170. Virtually all ROO–H BDEs are roughly 88 kcal/mol.
(8) DiLabio, G. A.; Pratt, D. A.; LoFaro, A. D.; Wright, J. S. *J. Phys. Chem. A* **1999**, *103*, 1653–1661.
(9) Curtiss, L. A.; Raghavachari, K.; Redfern, P. C.; Rassolov, V.; Pople, J. A. *J. Chem. Phys.* **1998**, *109*, 7764.
(10) Curtiss, L. A.; Redfern, P. C.; Raghavachari, K.; Rassolov, V.; Pople, J. A. *J. Chem. Phys.* **1999**, *110*, 4703–4709.
(11) Berkowitz, J.; Ellison, G. B.; Gutman, D. *J. Phys. Chem.* **1994**, *98*, 2744–2765.
(12) Trenwith, A. B. *J. Chem. Soc., Faraday Trans. 1* **1982**, *78*, 3131–3136. This C–H BDE, also measured by Clark et al. reference (Clark, K. B.; Culshaw, P. N.; Griller, D.; Lossing, F. P.; Martinho Simoes, J. A.; Walton, J. *J. Org. Chem.* **1991**, *56*, 5535–5539.) by photoacoustic calorimetry, was found to be 77 kcal/mol. However, upon revision of this value to 82 kcal/mol to correct for solvation (Laarhoven, L. J. J.; Mulder, P.; Wayner, D. D. M. *Acc. Chem. Res.* **1999**, *32*, 342–349), the authors admit that addition of *t*-BuO• to the double bond takes place under the experimental conditions, and the two processes cannot be deconvoluted, leading to an artificially high C–H BDE. Hence, we consider the older gas phase thermolysis value obtained by Trenwith to be most reliable.
(13) Pedley, J. B.; Naylor, R. D.; Kirby, S. P. *Thermochemical Data of Organic Compounds*, 2nd ed.; Chapman and Hall: London, 1986.
(14) Pratt, D. A.; de Heer, M. I.; Mulder, P.; Ingold, K. U. *J. Am. Chem. Soc.* **2001**, *123*, 5518–5526.
(15) Pratt, D. A.; DiLabio, G. A.; Brigati, G.; Pedulli, G. F.; Valgimigli, L. *J. Am. Chem. Soc.* **2001**, *123*, 4625–4626.
(16) Pratt, D. A.; DiLabio, G. A.; Valgimigli, L.; Pedulli, G. F.; Ingold, K. U. *J. Am. Chem. Soc.* **2002**, *124*, 11085–11092.
(17) Wright, J. S.; Johnson, E. R.; DiLabio, G. A. *J. Am. Chem. Soc.* **2001**, *123*, 1173–1183.
(18) Montgomery, J. A., Jr.; Ochterski, J. W.; Petersson, G. A. *J. Chem. Phys.* **1994**, *101*, 5900. Ochterski, J. W.; Petersson, G. A.; Montgomery, J. A., Jr. *J. Chem. Phys.* **1996**, *104*, 2598.
(19) It should be pointed out that the B3LYP-HLM C–H BDE for 1,3-pentadiene is in good agreement with the experimental, G3, and G3MP2 values despite the fact that the pentadienyl radical formed upon C–H homolysis is the same as that for 1,4-pentadiene. This suggests that the observation that DFT underestimates X–H BDEs (X = O, N) for compounds with increasingly weak bonds is not because of a problem with how the open shell radical is handled but instead the closed-shell precursor.

Table 1. C−H BDEs in Methane, Toluene, Propene, and Pentadiene by Various Levels of Theory[i]

method	CH₃−H	C₆H₅CH₂−H	CH₂=CHCH₂−H	(CH₂=CH)₂CH−H[g]
B3LYP-LLM[a]	105.5 (0.0)	89.3 (−16.2)	86.9 (−18.6)	71.9 (−33.6), *80.7 (−24.8)*
B3LYP-MLM1[b]	105.5 (0.0)	89.4 (−16.1)	87.1 (−18.4)	72.6 (−32.9), *80.8 (−24.7)*
B3LYP-MLM2[c]	105.5 (0.0)	90.1 (−15.4)	87.9 (−17.6)	74.1 (−31.4), *82.0 (−23.5)*
B3LYP-HLM[d]	105.8 (0.0)	90.6 (−15.2)	88.1 (−17.7)	74.2 (−31.6), *82.3 (−23.5)*
G3	104.9 (0.0)	91.1 (−13.8)	87.5 (−17.4)	75.6 (−29.3), *82.1 (−22.8)*
G3MP2	105.3 (0.0)	93.1 (−12.2)	88.6 (−16.7)	77.3 (−28.0), *83.7 (−21.6)*
experiment	104.9 ± 0.1[e] (0.0)	88.5 ± 1.5[e] (−16.4)	88.2 ± 2.1[e] (−16.7)	76.4[f] (−28.5), *83.5 (−21.4)[h]*

[a] (RO)B3LYP/6-311+G(2d,2p)//AM1/AM1. [b] (RO)B3LYP/6-311+G(2d,2p)//(U)MP2/6-31G(d)/(U)HF/6-31G(d). [c] (RO)B3LYP/6-311+G(2d,2p)//(U)B3LYP/6-31G(d). [d] (RO)B3LYP/6-311+G(2d,2p)//(U)B3LYP/6-311+G(2d,2p). [e] Reference 11. [f] Reference 12. [g] Values in italics for 1,3-pentadiene. [h] Obtained from the value for 1,4-pentadiene correcting for the difference in heats of formation between 1,4- and 1,3-pentadiene (7.1 kcal/mol); see ref 13. [i] RSEs are included in parentheses. All values in kcal/mol.

Table 2. Spin Distribution in Allyl, Benzyl and Pentadienyl by Various Levels of Theory

Method[a]	C1 : C3	C1 : ortho : para	C1 : C3 : C5
A	1 : 1	1.28 : 1.01 : 1	1 : 1.01 : 1
B	1 : 1	1.39 : 1 : 1.01	1 : 1.07 : 1
C	1 : 1	3.08 : 1 : 1.11	1 : 1.04 : 1
D	1 : 1	3.22 : 1 : 1.15	1 : 1.06 : 1
Expt.	1 : 1	3.19 : 1 : 1.22[b]	1 : 1.16 : 1[c]

[a] Methods: (A) UHF/6-31G(d); (B) UMP2/6-31G(d); (C) UB3LYP/6-311+G(2d,2p); (D) UB3P86/6-311G(d,p). [b] Taken from ref 23. [c] Taken from ref 24.

of a kilocalorie, theory predicts RSE(benzyl) < RSE(allyl) by 2.2−2.5 (DFT) and 3.6−4.5 (G3) kcal/mol, respectively. This is consistent with earlier theoretical calculations by Borden and Hrovat.[20] Some of our own kinetic measurements suggest that this difference is ∼2 kcal/mol.[21]

Upon C−H bond breaking, propene, toluene, and 1,4-pentadiene give rise to delocalized allyl, benzyl, and pentadienyl radicals, respectively, as shown in Table 2, and we have calculated the spin distribution in these radicals. The calculated values are compared to the relative spin density distribution as derived from the α-hyperfine coupling constants (α-hfcc's) obtained by EPR in Table 2.[22]

In the allyl radical, all four methods agree that the spin is distributed evenly between C1 and C3 as symmetry requires. In the pentadienyl radical, which also possesses C_{2v} symmetry, all of the theoretical methods suggest a slight bias for spin at the central carbon atom (C3), but by varying amounts, and in all cases, it is slightly underestimated relative to the EPR experiment. For the benzyl radical, the calculated spin densities by the DFT methods are in good agreement with the experimental values, but the HF and MP2 calculated spin densities differ substantially from the EPR experimental values. Experi-

ment (and DFT) values suggest that the sum of the spin density at the three ring positions is equal to the spin at the benzylic position, but HF and MP2 find that there is substantially more spin in the ring than at the benzylic position.

Where the B3LYP functional has been shown to underestimate X−X and X−Y (X,Y = non-hydrogen) BDEs, the B3P86 density functional has been found to be particularly useful for these purposes,[25] and thus, we have applied this to the series of peroxyl radicals formed upon addition of oxygen to the radicals shown in Table 2. We also include the unsubstituted methylperoxyl radical for comparison. Again, we also provide G3 and G3MP2 data for comparison. The results are shown in Table 3. Structures of the peroxyl radicals are shown in Figure 1. Details of alkylperoxyl radical structure provided by small basis HF/MP2 calculations[26] and DFT calculations[27] have been presented elsewhere.

For methylperoxyl, the G3 methods give the best agreement with experiment. B3P86-HLM overestimates the BDE by 1.4 kcal/mol, whereas B3P86-LLM and B3P86-MLM are in error by some 4.8 and 2.5 kcal/mol, respectively. For benzylperoxyl, SCF convergence difficulties with AM1, HF, and MP2 prevented the calculation of the C−OO• BDE by both the LLM and MLM B3P86 models as well as by G3 and G3MP2. B3P86-HLM has no convergence problems and provides a BDE in excellent agreement with experiment. For allylperoxyl and pentadienylperoxyl, all methods give results that are in reasonably good agreement with experiment. It is interesting to note that the difference between the HLM-calculated C−OO• BDEs for allylperoxyl and benzylperoxyl is 2.4 kcal/mol and the experimental value is 3.4 kcal/mol. This is consistent with the notion (*vide supra*) that the C−H BDE in toluene is indeed at least 2 kcal/mol higher than that in propene.

When the substituent effects on the C−OO• bond in methylperoxyl are calculated, shown in parentheses in Table 3, an initially unexpected trend results. We denote these substituent effects as apparent radical stabilization enthalpies, RSE*:

$$RSE^*(Y) = BDE(Y-CH_2-OO^\bullet) - BDE(CH_3-OO^\bullet) \quad (2)$$

Given that we are forming the same radicals (Table 2), whether we break the C−H bonds shown in Table 1 or the

(20) Hrovat, D. A.; Borden, W. T. *J. Phys. Chem.* **1994**, *98*, 10460−10464.
(21) The rate constant of β-fragmentation of the nonconjugated allylbenzylperoxyl radical to the allylbenzyl radical is 1 order of magnitude slower than the rate constant of β-fragmentation of the nonconjugated pentadienylperoxyl of methyl linoleate. Given the plots in Figures 5 and 6, we translate this to a difference in RSE of roughly 2 kcal/mol.
(22) Spin densities derived from unrestricted wave functions are reported. Although spin densities from restricted wave functions yielded spin distributions that follow the same trend as those from the unrestricted calculations, they do not reproduce experimental relative spin distributions as well. For example, the spin distribution in the benzyl radical from a ROB3LYP/6-311+G(2d, 2p) calculation places spin at the benzylic, ortho, and para positions in a ratio of 5.31:1:1.27.
(23) Dust, J. M.; Arnold, D. R. *J. Am. Chem. Soc.* **1983**, *105*, 1221−1227.
(24) Davies, A. G.; Griller, D.; Ingold, K. U.; Lindsay, D. A.; Walton, J. C. *J. Chem. Soc., Perkin Trans. 2* **1981**, 633.
(25) DiLabio, G. A.; Pratt, D. A. *J. Phys. Chem. A* **2000**, *104*, 1938−1943.
(26) Boyd, S. L.; Boyd, R. J.; Shi, Z.; Barclay, L. R. C.; Porter, N. A. *J. Am. Chem. Soc.* **1993**, *115*, 687−693.
(27) Kranenburg, M.; Ciriano, M. V.; Cherkasov, A.; Mulder, P. *J. Phys. Chem. A* **2000**, *104*, 915−921.

Table 3. C−OO• BDEs in Methylperoxyl, Benzylperoxyl, Allylperoxyl, and 1-Pentadienylperoxyl by Various Levels of Theory[i]

| method	CH_3−OO•	$C_6H_5CH_2$−OO•	CH_2=$CHCH_2$−OO•	CH_2=$CHCH$=CH−CH_2−OO•
B3P86-LLM[a]	37.2 (0.0)	h	20.6 (−16.6)	15.3 (−21.9)
B3P86-MLM[b]	35.9 (0.0)	h	21.2 (−14.7)	15.0 (−20.9)
B3P86-HLM[c]	34.1 (0.0)	22.2 (−11.9)	19.8 (−14.3)	14.0 (−20.1)
G3MP2	32.4 (0.0)	h	19.7 (−12.7)	15.1 (−17.3)
G3	32.2 (0.0)	h	19.0 (−13.2)	13.9 (−18.3)
experiment	32.7 ± 0.9 (0.0)[d]	21.8 ± 0.9 (−10.9)[e]	18.4 ± 0.6 (−14.3)[f]	13.4 ± 1.2 (−19.3)[g]

[a] (RO)B3P86/6-311G(d,p)//AM1/AM1. [b] (RO)B3P86/6-311G(d,p)//(U)MP2/6-31G(d)/(U)HF/6-31G(d). [c] (RO)B3P86/6-311G(d,p)//(U)B3P86/-6311G(d,p). [d] Reference 28. [e] Reference 29. [f] Reference 30. [g] Reference 31. [h] SCF failed to converge (QC as well). [i] RSE*'s are included in parentheses (see text). All values in kcal/mol.
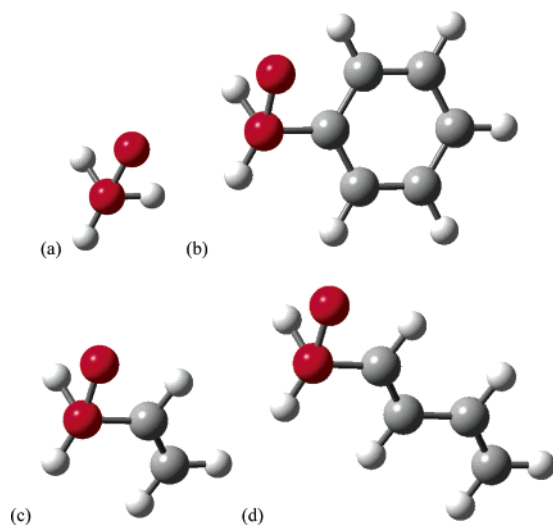
Figure 1. Minimum energy conformations of (a) methylperoxyl, (b) benzylperoxyl, (c) allylperoxyl, and (d) pentadienylperoxyl. View shown looking down the peroxyl C−O bond.

C−OO• bonds in Table 3, we would expect that the effect of substituents on the C−H or C−OO• BDE would be the same. We find that this is not the case. In fact, RSE* < RSE in all cases. For example, with the HLM methodologies, (RSE − RSE*) = 3.3 (phenyl), 3.4 (vinyl), and 3.4 (dienyls) kcal/mol, respectively. The corresponding experimental values are 5.5, 2.4, and 2.1, kcal/mol, respectively. This unexpected result is due to negative hyperconjugation of the filled π-HOMO of the benzylic/vinylic/dienylic substitutent and the empty $\sigma_{C−O}$* of the alkylperoxyl radical:[32]
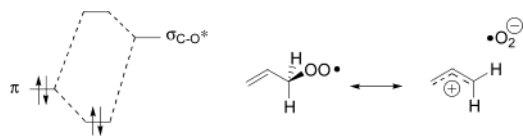
Since both of the DFT-HLM models perform well in predicting the relative spin density distribution in delocalized radicals, the BDEs of the C−H bonds that are broken to form these radicals and the BDEs of the C−OO• bonds formed upon addition of oxygen to these radicals, we have confidence that calculated results with these methods for lipids of biological relevance reasonably reflect reality. The unsaturated lipids we have studied are shown in Figure 2.
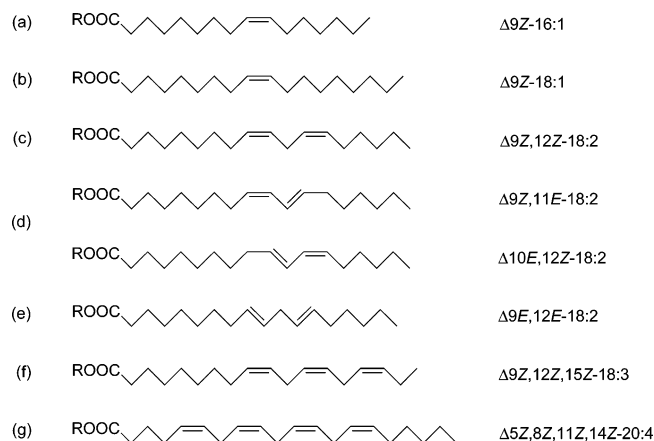
Figure 2. Lipids of interest: (a) palmitoleate, (b) oleate, (c) linoleate, (d) conjugated linoleate, (e) linoleidate, (f) linolenate, (g) arachidonate.

Table 4. Spin Distributions in Isomers of the 1,3-Dimethylallyl and 1,5-Dimethylpentadienyl Radicals by Various Levels of Theory

Method[a]	Entry 1	Entry 2	Entry 3	Entry 4	Entry 5
	C2 : C4	C2 : C4[c]	C2 : C4 : C6[d]	C2 : C4 : C6[e]	C2 : C4 : C6[f]
A	1 : 1	1.01 : 1	1 : 1.04 : 1	1.01 : 1.05 : 1	1 : 1.04 : 1
B	1 : 1	1.05 : 1	1 : 1.10 : 1	1.02 : 1.12 : 1	1 : 1.10 : 1
C	1 : 1	1.04 : 1	1 : 1.09 : 1	1.08 : 1.18 : 1	1 : 1.15 : 1
D	1 : 1	1.03 : 1	1 : 1.10 : 1	1.05 : 1.14 : 1	1 : 1.11 : 1
Expt.[b]	1 : 1	1.15 : 1	1 : 1.13 : 1	1.09 : 1.23 : 1	1 : 1.23 : 1

[a] Methods: (A) UHF/6-31G(d); (B) UMP2/6-31G(d); (C) UB3LYP/6-311+G(2d,2p); (D) UB3P86/6-311G(d,p). [b] Derived from hyperfine coupling constants taken from ref 34. [c] Oleate/palmitoleate model. [d] Linoleate/linolenate/arachidonate model. [e] Conjugated linoleates model. [f] Linoleidate model.

C−H BDEs in Lipids, Spin Distributions in Lipid Radicals, and C−OO• BDEs in Lipid Peroxyls. It seems reasonable to suggest that oxygen addition to delocalized radicals is related to the spin distribution in the radical.[34] We therefore considered the spin density distribution in the delocalized radicals formed from hydrogen atom abstraction at the activated (allylic or bis-allylic) positions of precursor lipids. The results of these calculations are shown in Table 4.

Entry 2 of Table 4 shows the spin density distribution in the cis−trans allyl radical generated from removal of an oleate allylic hydrogen. The calculations all suggest that there is greater spin density at the cisoid end of this radical compared to the

(28) Knyazev, V. D.; Slagle, I. R. *J. Phys. Chem. A* **1998**, *102*, 1770−1778.
(29) Fenter, F. F.; Noziere, B.; Caralp, P.; Lesclaux, R. *Int. J. Chem. Kinet.* **1994**, *26*, 171.
(30) Knyazev, V. D.; Slagle, I. R. *J. Phys. Chem. A* **1998**, *102*, 8932−8940.
(31) Zils, R.; Inomata, S.; Imamura, T.; Miyoshi, A.; Washida, N. *J. Phys. Chem. A* **2001**, *105*, 1277−1282.
(32) Pratt, D. A.; Porter, N. A. *Org. Lett.* **2003**, *5*, 387−390.

(33) Porter, N. A.; Mills, K. A.; Carter, R. L. *J. Am. Chem. Soc.* **1994**, *116*, 6690−6696.
(34) Bascetta, E.; Gunstone, F. D.; Walton, J. C. *J. Chem. Soc., Perkin Trans. 2* **1983**, 603−613.

Table 5. C–OO• BDEs in Model Peroxyl Radicals Formed in the Autoxidation of Oleates, Linoleates, and Their Isomers (C–H BDEs Are Presented for Comparison)

entry		X=OO•		X=H
		B3P86-HLM (kcal/mol)	k_β (s^{-1})	B3LYP-HLM (kcal/mol)
1.		19.6	3[a]	83.4[e]
2.		23.1	--	87.0
3.		20.5	8[a]	84.0
4.		21.3	0.5[a]	84.9
5.		7.4	2.4×10^6 [b,d]	72.7[f]
6.		7.9	3.1×10^6 [d]	73.1
7.		8.4	2.6×10^6 [d]	73.5[h]
8.		15.3	27[c]	78.5
9.		14.2	430[c]	77.4[g]
10.		14.6	--	77.7
11.		15.7	--	78.8

[a] Taken from ref 33. [b] Taken from ref 6b. [c] Taken from ref 5. [d] Unpublished results. [e] Oleate/palmitoleate model. [f] Linoleate/linolanate/arachidonate model. [g] Conjugated linoleates model. [h] Linoleidate model.

transoid end and the EPR hfcc's[34] are consistent with this conclusion. The calculations and EPR both suggest that there should be a preference for oxygen addition at the cisoid end of the radical. In the case of oleate oxidation,[33] 45% of oxygen adds at the transoid end of the intermediate cis–trans allyl radical, whereas 55% of oxygen addition occurs at the cisoid end of the radical. This result suggests that oxygen adds preferentially to carbon centers in delocalized radicals that bear the highest spin density.

The radical shown in entry 3 of Table 2 is the first-formed carbon radical in the oxidation of linoleic acid or linoleate esters. All of the calculations reported in the table for this radical indicate that C4 bears the highest spin density of any of the carbons, and EPR results support this conclusion. Oxidation of linoleate esters in the presence of high concentrations of α-tocopherol gives products in which 43% of oxygen addition occurs at the C4 carbon while 27% of oxygen addition occurs at each of the cisoid carbons at C2 and C6. Again, the results support the notion that oxygen addition occurs preferentially at sites of the highest spin density in a delocalized radical.

The unsymmetrical radical shown in entry 4 of Table 2 would be formed in the oxidation of a Z,E isomer of linoleate. The calculations all predict an even higher spin density at C4 of this radical than is the case for the radical formed from linoleate, which has a Z,Z alkene configuration. EPR experiments are consistent with this result. Oxidation reactions of the Z,E isomer have been reported but these studies were not carried out in the presence of high concentrations of α-tocopherol, and the results therefore do not reflect the kinetically controlled product distribution. Indeed, no products resulting from oxygen addition at C4 were observed, and none would be expected under the low H atom donor conditions of oxidation used. We are currently examining the oxidation of the Z,E and E,E linoleate isomers under conditions where high concentrations of antioxidants are present, and the results of these studies will be reported elsewhere. Suffice it to say that we do indeed observe preferential addition of oxygen at C4 of these radicals under kinetically controlled oxidation conditions.

Theory provides guidance in predicting the sites of addition of oxygen to delocalized radicals (*vide supra*), and we anticipate that calculations of the relevant C–H and C–OO• BDEs would have predictive value for the rates of propagation for the slow chain step, k_p, and β-fragmentation of intermediate peroxyls, k_β. The results of these calculations are presented in Table 5,
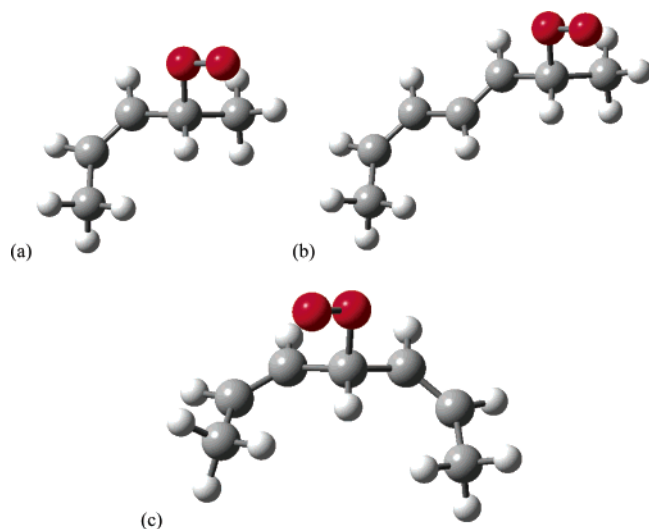
Figure 3. Minimum energy structures of the (a) oleate peroxyl radical model, Table 5, entry 1; (b) conjugated linoleate peroxyl radical model, Table 5, entry 8; and (c) nonconjugated linoleate peroxyl radical model, Table 5, entry 5.

and minimum energy structures of representative peroxyl radicals are shown in Figure 3.

As might be expected, there is a correlation of calculated $C-OO^\bullet$ BDEs and $C-H$ BDEs derived from analogous structures. Lipid molecules that have weak $C-H$ bonds generally correspond to peroxyl radicals that have weak $C-OO^\bullet$ bonds, since the same carbon radicals are formed upon bond breaking. Of more practical interest is the correlation of the $C-H$ and $C-OO^\bullet$ BDEs with the important reactions that they undergo in free radical chain oxidation. Molecules that have low $C-H$ BDEs have high rates for hydrogen atom abstraction by a peroxyl radical. Since this step is usually the slow step in autoxidation, Scheme 1, it is of some interest to consider in more detail the relationship between the calculated $C-H$ BDEs and experimentally determined k_p's for autoxidation. The experimental rates of hydrogen atom transfer to peroxyl radicals are plotted versus the DFT-calculated $C-H$ BDEs of the hydrocarbon precursor in Figure 4. The correlation is only satisfactory, $R^2 = 0.816$, which is not surprising given the fact that the experimental values of k_p are obtained with difficulty and have significant associated error. Most of the rate constants used to generate Figure 4 come from the rotating sector method, as implemented by Howard and Ingold,[35] requiring that rates of termination and initiation be determined as well as the rate of substrate or oxygen consumption. Based upon this analysis, the best fit of the data is described by eq 3. This equation provides predictions of propagation rate constants for substrates for which this value is not known. Given the difficulty associated with the experimental determination of such rate constants, we believe eq 3 may prove to be of some value.[36]

$$\log k_p = -0.219(C-H\ BDE) + 18.9 \qquad (3)$$

Peroxyl radicals having low $C-OO^\bullet$ BDEs also have high rate constants for β-fragmentation, although the set of rate constants available for comparison is rather small. In fact, β-fragmentation rates have only been reported for peroxyl radicals derived from oleates and linoleates, allylperoxyl,

(35) Howard, J. A. *Adv. Free Radical Chem.* **1972**, *4*, 49−173.
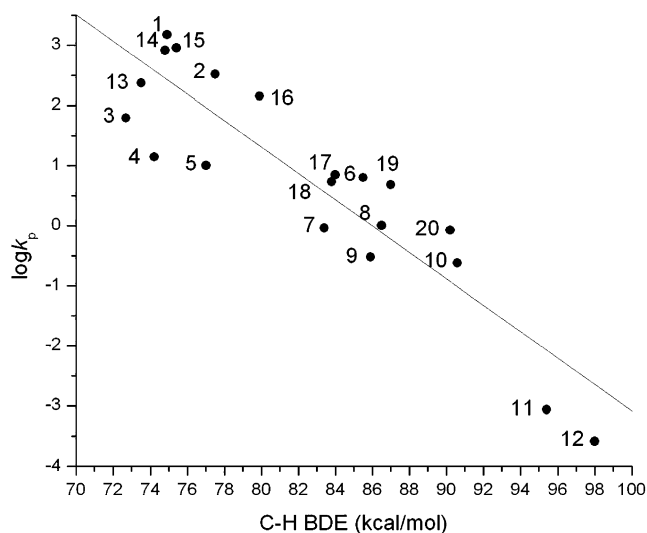
Figure 4. Logarithm of experimental rate constants for chain propagation in the autoxidation of various hydrocarbons ((**1**) 1,4-cyclohexadiene; (**2**) 9,10-dihydroanthracene; (**3**) linoleate; (**4**) 1,4-pentadiene; (**5**) allylbenzene; (**6**) tetralin; (**7**) oleate; (**8**) ethylbenzene; (**9**) cumene; (**10**) toluene; (**11**) cyclopentane; (**12**) cyclohexane; (**13**) linolenate; (**14**) 1,3-cyclohexadiene; (**15**) 1,4-dihydronaphthalene; (**16**) indene; (**17**) cyclohexene; (**18**) cyclopentene; (**19**) indan; (**20**) *p*-xylene) plotted as a function of calculated $C-H$ BDEs. Chain propagation rate constants are taken from ref 35.
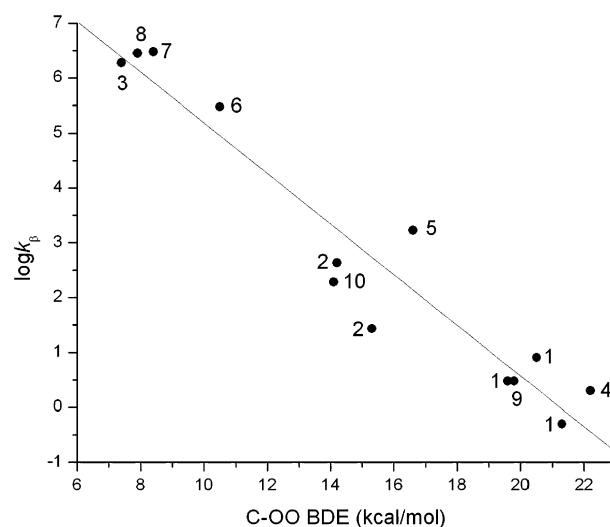
Figure 5. Logarithm of experimental rate constants for β-fragmentation of lipid peroxyls ((**1**) oleate peroxyl radicals, ref 33; (**2**) conjugated linoleate peroxyl radicals, ref 5; (**3**) nonconjugated linoleate peroxyl radical, ref 6b; (**4**) cumylperoxyl radical, ref 37; (**5**) diphenylethylperoxyl radical, ref 38; (**6**) α-vinyl benzylperoxyl radical, unpublished results; (**7**) nonconjugated linoleiadate peroxyl radical, unpublished results; (**8**) nonconjugated cis/trans linoleate peroxyl radical, unpublished results; (**9**) allylperoxyl radical, ref 30; (**10**) conjugated pentadienylperoxyl, ref 31) plotted as a function of calculated $C-OO^\bullet$ BDEs.

cumylperoxyl, diphenylperoxyl, and pentadienylperoxyl. In addition, we have recently measured k_β for α-vinyl benzylperoxyl, **6**, in our laboratory. The experimental rate constants of β-fragmentation are plotted versus the DFT-calculated $C-OO^\bullet$ BDEs in Figure 5. A linear correlation is obtained with an $R^2 = 0.923$. Given that the rate constants for β-fragmentation span 7 orders of magnitude and were obtained over a period of more than 20 years and by very different methods, we find that it is perhaps not surprising that the correlation is not better. Based upon this analysis, eq 4 best describes the relationship between k_β and the calculated $C-OO^\bullet$ BDE.[39]

$$\log k_\beta = -0.46(\text{C}-\text{OO}^\bullet \text{ BDE}) + 9.8 \qquad (4)$$

BDEs and Secondary Oxidation of Arachidonate and Linolenate. All six of the primary oxidation products of arachidonate and two of the four primary oxidation products of linolenate are lipid hydroperoxides that have activated methylene groups with very weak C−H bonds (*vide infra*). Scheme 3 shows the primary and secondary oxidation pathways of arachidonate.

To provide predictions about the propensity of primary oxidation products shown in Scheme 3 to undergo further oxidation and to provide predictions of the rate of fragmentation for individual peroxyl radicals, we have calculated the C−H and C−OO• BDEs of the structures shown in Table 6. Also presented in Table 6 are the calculated k_β for the loss of oxygen from the peroxyl as well as the k_p calculated for H atom abstraction from a C−H precursor by a peroxyl radical.

Of particular note is that four of the six primary hydroperoxide products derived from arachidonate can undergo secondary oxidation to give a heptatrienyl radical, while two of the six give pentadienyl radicals upon secondary oxidation. Thus, four of the six primary oxidation products of arachidonate and two of four of linolenate are predicted to be more easily oxidized than arachidonate and linolenate themselves, since removal of a hydrogen can yield a heptatrienyl radical. When one compares the C−H BDE 69.8 kcal/mol for entry 1, Table 6 with 72.7 kcal/mol for entry 5, Table 5, it is predicted that k_p should increase by roughly a factor of 5. Clearly, secondary oxidation products will become a significant component of the oxidation mixture formed from a polyunsaturated lipid if oxidation of more than a few percent of the lipid takes place. Also of note is the fact that β-fragmentation of peroxyl radicals shown in Table 6 generally occurs at high rates. For example, the peroxyl radical shown in entry 1 of the table is an intermediate in one of the secondary oxidation pathways for arachidonate, and the rate constant for fragmentation of this peroxyl is such that it is unlikely that appreciable quantities of this peroxyl will be trapped, even with concentrations of 100 mM α-tocopherol (since $k = 3.8 \times 10^6$ M^{-1} s^{-1} for α-TOH + ROO•,[15] the rate of trapping by α-TOH will be 0.1 M × [ROO•] × (3.8 × 10^6 M^{-1} s^{-1}) = 3.8 × 10^5 s^{-1}[ROO•] compared to the rate of β-fragmentation, which will be 7.4 × 10^7 s^{-1}[ROO•]).

In the heptatrienyl radical shown in Scheme 3, positive spin density is found at four possible positions, with the inner positions (C4 and C6 in Table 7) possessing the greatest spin densities. This suggests that oxygen addition will occur pre-
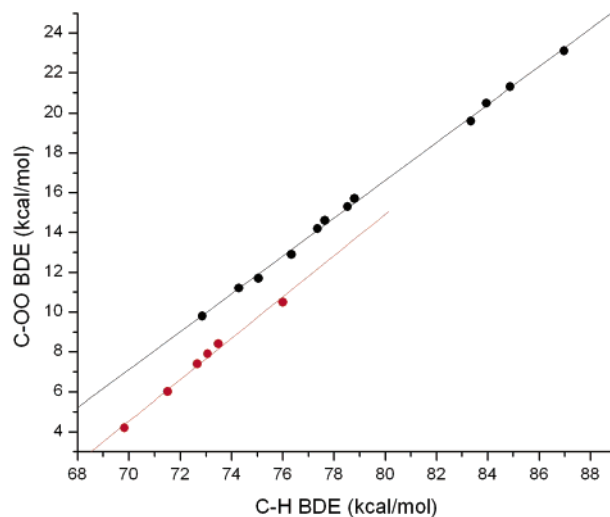
Figure 6. Calculated C−OO• BDEs of lipid peroxyls plotted as a function of C−H BDEs of corresponding lipids.

dominantly at these interior positions, and that the lipid hydroperoxides resulting from oxygen addition at these positions will be the kinetic products of lipid autoxidation.

Hyperconjugative Stabilization of Peroxyl Radicals. In Figure 6 is presented the calculated C−OO• BDE plotted versus the calculated C−H BDE for the substrates shown in Tables 5 and 6 (and allylbenzylperoxyl/allylbenzene). While one anticipates that these BDEs should be closely related, the plot shows that two different correlations exist for the data. The upper line corresponds to the data for the peroxyls having only one vinylic, conjugated dienylic or trienylic π system attached to the peroxyl α carbon, while the lower line corresponds to peroxyls that have two π systems (diene, triene, or arene) attached to the α center. Thus, it appears that there is an effect related to the local substructure of the peroxyl bearing carbon in addition to the more general correlation with radical stabilization enthalpy and conjugation in the parent lipid/peroxyl. If radical stabilization and parent conjugation were the only factors operating, one would not expect that two separate sets of data would be observed in Figure 6.

The importance of hyperconjugative stabilization in peroxyl radicals has been pointed out elsewhere,[32,27] and we suggest that this effect gives rise to the *two* correlations shown in Figure 6. The RSE for an allyl radical relative to a methyl radical is 16.7 (HLM: −17.7) kcal/mol, and one would therefore expect a C−OO• BDE in allylperoxyl of 32.7−16.7 = 16 (HLM: 34.1−17.7 = 16.4) kcal/mol. Instead, the C−OO• BDE is 18.4 (HLM: 19.8) kcal/mol. Thus, the hyperconjugative interaction between the σ_{C-O}^* and the HOMO of the vinyl group is worth approximately 2.4 (HLM: 3.4) kcal/mol. A similar analysis can be done for comparison for the ethylperoxyl radical. The RSE for an ethyl radical relative to a methyl radical is 3.8 (HLM: 4.8) kcal/mol, and one would expect a C−OO• BDE in ethylperoxyl of 32.7−3.8 = 28.9 (HLM: 34.1−4.8 = 29.3) kcal/mol. Instead, this BDE is known to be 35.5 (HLM: 35.1) kcal/mol, which makes for the interaction between the combination of σ_{C-H} and the σ_{C-O}^* of 6.6 (HLM: 5.8) kcal/mol. From this analysis, we conclude that a peroxyl bearing two π substitutents (no alkyl substitutents) would have a lower C−OO• BDE than that of such a radical bearing one π and one alkyl substituent, since alkyl substituents further stabilize the peroxyl radical. This

(36) It is worth noting that the propagating radical in autoxidations of cyclohexadienes, 9,10-dihydroanthracene, and 1,4-dihydronaphthalene was likely hydroperoxyl and that rate constants for cyclopentane and cyclohexane are for reactions with *t*-BuOO•. All rate constants are reported as measured and not on a per hydrogen basis.

(37) Howard, J. A.; Bennett, J. E.; Brunton, G. *Can. J. Chem.* **1981**, *59*, 2253−2260.

(38) Howard, J. A.; Chenier, J. H. B.; Yamada, T. *Can. J. Chem.* **1982**, *60*, 2566−2572.

(39) The kinetic approach to determine the linoleate values of k_β used in Figure 5 (entries in **2**) was based upon a competition of fragmentation of the linoleate peroxyl radicals and H-atom abstraction from 1,4-cyclohexadiene by these radicals. The value of the rate constant for H-atom abstraction used for comparison was k_p (1,4-CHD) 270 M^{-1} s^{-1} in co-oxidations with cyclohexadiene, whereas the values measured by Howard and Ingold for this rate constant are closer to 1400. Taking this difference into consideration, roughly a factor of 5 in the rate constant, we observe the corrected linoleate points now give rise to an overall $R^2 = 0.946$ in the plot in Figure 5. We nevertheless use the "uncorrected" eq 5 as a means to make predictions of k_β of peroxyl radicals for which the rate constant is unknown, since the overall line of best fit does not really change: $\log k_\beta = -0.46$-(C−OO• BDE) + 9.9.

Scheme 3. Arachidonate Primary and Secondary Oxidation Pathways

heptatrienyl radical
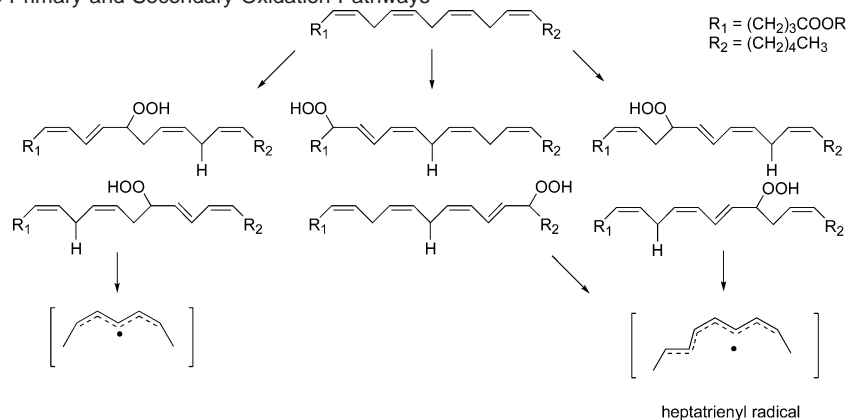
Table 6. C−OO• BDEs for Peroxyl Radicals Formed from Secondary Arachidonate Oxidation and C−H BDEs in Their Corresponding Lipid Precursors[a]

entry		X=OO•		X=H	
		B3P86-HLM (kcal/mol)	k_β [a] (s^{-1})	B3LYP-HLM (kcal/mol)	k_p [b] (M^{-1}s^{-1})
1		4.2	7.4×10^7	69.8	4.1×10^3
2		6.0	1.1×10^7	71.5	1.7×10^3
3		11.2	4.4×10^4	74.3	420
4		9.8	2.0×10^5	72.9	860
5		12.9	7300	76.3	150
6		11.7	2.6×10^4	75.1	280

[a] Predicted based upon eq 4. [b] Predicted based upon eq 3.

Table 7. Spin Distribution in 1,7-Dimethylheptatrienyl by Various Levels of Theory

Method[a]	C2 : C4 : C6 : C8
A	1 : 1.08 : 1.08 : 1.03
B	1 : 1.22 : 1.23 : 1.08
C	1 : 1.47 : 1.47 : 1.32
D	1 : 1.45 : 1.46 : 1.27

[a] Methods: (A) UHF/6-31G(d); (B) UMP2/6-31G(d); (C) UB3LYP/6-311+G(2d,2p); (D) UB3P86/6-311G(d,p).

difference in hyperconjugation in the peroxyl C−OO• BDEs is expected to be approximately equal to the difference between the vinyl and methyl stabilization, 6.6−2.4 = 4.2 (HLM: 5.8−3.4 = 2.4) kcal/mol, in reasonable agreement with the difference of ∼2−2.5 kcal/mol between the data on the two lines in Figure 6.

Lipids with Extended Conjugation. Extending conjugation makes the rates of propagation and β-fragmentation faster (for both the conjugated and nonconjugated peroxyl radicals), as shown for the comparison of the monoene, diene, and triene systems described in Tables 5 and 6. Figure 7 shows the calculated C−OO• BDEs in structures having extended conjugation. This leads to peroxyl radicals with nonconjugated π systems having C−OO• BDEs of 2.4 and 1.3 kcal/mol, for the tetraene (n=3) and pentaene (n=4) peroxyls, respectively. Application of eq 4 suggests that the rate constants for β-fragmentation of these peroxyls would be 5.0×10^8 and 1.6×10^9 s^{-1}. Products formed from oxygen addition at these centers would likely never be observed because of these extremely rapid oxygen off-rates. For peroxyl radicals having only conjugated π systems, the C−OO• BDE, and the rate of β-fragmentation, levels off with extended conjugation, approaching a value of 10^5 s^{-1}. We conclude that products resulting from oxygen addition to these radicals may be observed but only at the terminal (conjugated) positions. Such radicals can be generated from, for example, the oxidation of carotenoids.[40]
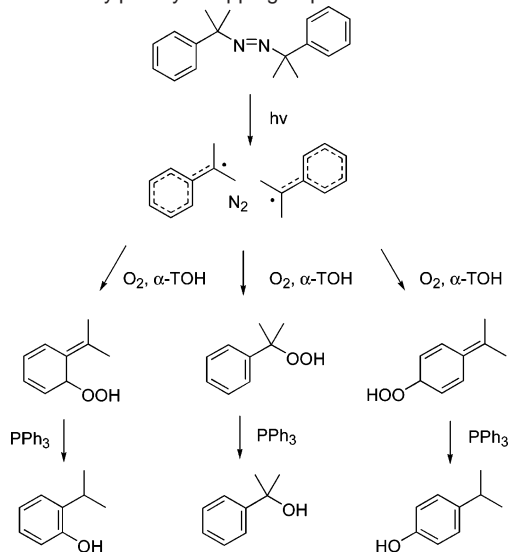
Peroxyls Derived from Benzylic Radicals. Table 2 shows that the spin density distribution in benzyl radicals places
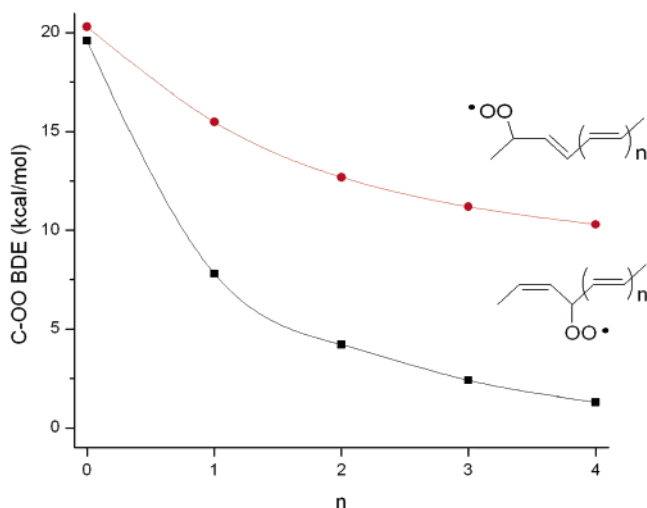
Figure 7. C−OO• BDEs in lipid peroxyls as a function of double bond number.

Scheme 4. Cumylperoxyl Trapping Experiments

significant spin in the aromatic ring, and this suggests that nonaromatic quinoid type peroxide products might form from these radicals. A critical issue in this chemistry revolves around the lifetime of these quinoid peroxyls. If they live long enough to be trapped by a good H-atom donor such as α-tocopherol, they should be found as a significant part of the product mixture.

Several experiments were carried out with the intent of trapping the kinetic product mixture of oxygen addition to cumyl radicals. For these trapping experiments, we used cumylperoxyl radicals generated photolytically from azocumene in the presence of oxygen and α-TOH. All efforts to find evidence of ring oxygen addition to cumyl radicals failed, the only peroxide observed in these experiments being cumyl hydroperoxide. Quenching these reactions with triphenylphosphine, expecting cumyl alcohol, and the two phenols 2-isopropylphenol and 4-isopropylphenol, which would form by aromatization of the quinoid alcohols, also provided no evidence for their formation.

(40) Burton, G. W.; Ingold, K. U. *Science* **1984**, *224*, 569. It has been suggested that β-carotene reacts with peroxyl radicals by addition to form a delocalized carbon-centered radical, which does not add oxygen and carry the chain. Although it is well-documented that addition occurs to give an intermediate carotenoid carbon radical, the fate of this radical remains unclear.

Only cumyl alcohol could be detected. These reactions are summarized in Scheme 4.

Calculation of the C−OO• BDEs for the quinoid peroxyl radicals provides an estimate of the rate constant for β-fragmentation of these peroxyls. The calculated C−OO• BDEs for the ortho and para addition products of −8.1 and −6.4 kcal/mol, respectively, indicate that the rate constant for β-fragmentation will exceed even the diffusion-controlled limit for a bimolecular reaction, that is, $k_{\beta,ortho} = 3.4 \times 10^{13}$ s^{-1} and $k_{\beta,para} = 5.5 \times 10^{12}$ s^{-1} from eq 4, thus approaching the kinetic limit for this kind of unimolecular reaction. Experiments to detect products derived from quinoid peroxyls were bound to fail.

Summary

1. DFT can be used to calculate C−H and C−OO• BDEs to a reasonable level of accuracy and to predict the relative spin distribution in delocalized radicals.

2. DFT-calculated C−H BDEs correlate with experimental rate constants for chain propagation for autoxidation. C−OO• BDEs correlate with experimental rate constants for the β-fragmentation of lipid peroxyl radicals.

3. C−OO• BDEs and k_β values of lipid peroxyl radicals are determined largely by the conjugative stability of the parent peroxyl as well as the radical stabilization of the carbon-centered radical. Hyperconjugation may also play a role.

4. The primary oxidation products of arachidonate and linolenate are more oxidizable than the parent lipids themselves. The values of k_β for the peroxyl radicals formed in secondary oxidation, which would be very difficult to elucidate experimentally, can be predicted by eq 4. These predicted rate constants may help in the mechanistic deconvolution of the complex product mixtures that result from the autoxidation of highly unsaturated lipids.

5. Extending conjugation increases k_β's. These rates appear to level off at about 10^5 for peroxyl radicals having only one π system attached to the carbon bearing the peroxyl, and they increase to 10^9 for peroxyl radicals having two π systems attached to this carbon.

6. Quinoid peroxyl radicals formed from ring addition of oxygen to benzylic radicals have negative BDEs and thus cannot be trapped.

Experimental Section

Theoretical Calculations. Geometries were optimized and vibrational frequencies calculated using either B3LYP/6-311+G(2d,2p) (C−H BDEs)[8] or B3P86/6-311G(d,p) (C−OO BDEs)[25] as implemented in the Gaussian 98[41] suite of programs compiled to run on an SGI Origin. Vibrational frequencies were scaled by 0.9806, as suggested by Scott and Radom.[42] After enthalpic corrections of the energy to 298 K, the enthalpies of products and reactants of the bond homolysis (either

(41) Frisch, M. J.; Trucks, G. W.; Schlegel, H. B.; Scuseria, G. E.; Robb, M. A.; Cheeseman, J. R.; Zakrzewski, V. G.; Montgomery, J. A., Jr.; Stratmann, R. E.; Burant, J. C.; Dapprich, S.; Millam, J. M.; Daniels, A. D.; Kudin, K. N.; Strain, M. C.; Farkas, O.; Tomasi, J.; Barone, V.; Cossi, M.; Cammi, R.; Mennucci, B.; Pomelli, C.; Adamo, C.; Clifford, S.; Ochterski, J.; Petersson, G. A.; Ayala, P. Y.; Cui, Q.; Morokuma, K.; Malick, D. K.; Rabuck, A. D.; Raghavachari, K.; Foresman, J. B.; Cioslowski, J.; Ortiz, J. V.; Baboul, A. G.; Stefanov, B. B.; Liu, G.; Liashenko, A.; Piskorz, P.; Komaromi, I.; Gomperts, R.; Martin, R. L.; Fox, D. J.; Keith, T.; Al-Laham, M. A.; Peng, C. Y.; Nanayakkara, A.; Gonzalez, C.; Challacombe, M.; Gill, P. M. W.; Johnson, B.; Chen, W.; Wong, M. W.; Andres, J. L.; Gonzalez, C.; Head-Gordon, M.; Replogle, E. S.; Pople, J. A. *Gaussian 98*, revision A.7; Gaussian, Inc., Pittsburgh, PA, 1998.
(42) Scott, A. P.; Radom, L. *J. Phys. Chem.* **1996**, *100*, 16502.

R−H → R• + H• or ROO• → R• + O$_2$) were differenced to give the bond dissociation enthalpy (BDE) at 298 K. Where possible, the high accuracy G3 and/or G3MP2 compound methods were employed for comparison.

Cumylperoxyl Trapping Experiments. Azocumene was synthesized using the method of Nelsen and Bartlett.[43] Reactions were conducted in 1 dram Teflon capped vials. Total reaction volumes were 100 μL, and the solvent was benzene. The concentration of azocumene was 0.05 or 0.1 M, and α-tocopherol concentrations ranged from 0.1 to 0.75 M. Thermolysis of the azo compound was carried out at 55 and 65 °C from 8 to 30 h, and photolysis was with a 400 W medium pressure mercury lamp in a quartz cuvette overnight. All products (hydroperoxide, alcohol, and phenols; see Scheme 4) were commercially available and were purchased from Aldrich Chemical Co. to be used as authentic standards. Analysis of hydroperoxide products was by normal phase HPLC with UV detection at 254 nm using a 0.3% isopropyl alcohol/hexane solvent system.

(43) Nelsen S. F.; Bartlett, P. D. *J. Am. Chem. Soc.* **1966**, *88*, 137−143.

In some experiments, hydroperoxide products were immediately reduced by triphenylphosphine before analysis by GC on an SPB-1 capillary column. The reduction was performed by adding a crystal of triphenylphosphine to the reaction mixture after oxidation. A crystal of BHT was also added as a stabilizer. The only oxygen-containing products observed under any conditions of azocumene decomposition were cumyl hydroperoxide and cumyl alcohol.

Supporting Information Available: Cartesian coordinates and thermochemical data for all computed structures. This material is available free of charge via the Internet at http://pubs.acs.org.

JA034182J